Chinese Chemical Letters 35 (2024) 108972

Contents lists available at ScienceDirect

Chinese Chemical Letters

journal homepage: www.elsevier.com/locate/cclet

Controlling molecular assembly on time scale: Time-dependent multicolor fluorescence for information encryption

Zixi Zou[1], Jingyuan Wang[1], Yian Sun[1], Qian Wang*, Da-Hui Qu*

Key Laboratory for Advanced Materials and Feringa Nobel Prize Scientist Joint Research Center, School of Chemistry and Molecular Engineering, East China University of Science and Technology, Shanghai 200237, China

ARTICLE INFO

Article history:
Received 2 June 2023
Revised 23 August 2023
Accepted 24 August 2023
Available online 27 August 2023

Keywords:
Supramolecular chemistry
Multicolor fluorescence
White light emission
Time-dependent fluorescence
Information encryption

ABSTRACT

Dynamic assembly on time scale is common in biological systems but rare for artificial materials, especially for smart luminescent materials. Programming molecular assembly in a spatio-temporal manner and resulting in white-light-including multicolor fluorescence with time-dynamic features remains challenging. Herein, controlling molecular assembly on time scale is achieved by integrating a pH-responsive motif to a transient alkaline solution which is fabricated by activators (NaOH) and deactivators (esters), leading to automatic assembly on time scale and time-dependent multicolor fluorescence changing from blue to white and yellow. The kinetics of the assembly process is dependent on the ester hydrolysis process, which can be controlled by varying ester concentrations, temperature, initial pH, stirring rate and ester structures. This dynamic fluorescent system can be further developed for intelligent fluorescent materials such as fluorescent ink, three-dimension (3D) codes and even four-dimension (4D) codes, exhibiting a promising potential for information encryption.

Organic multicolor luminescent materials, especially those displaying white light emission, have attracted considerable attention in recent years owing to their broad application in biology, display devices, and material science [1–7]. How to tailor luminescent properties is therefore becoming a key research objective. The discovery of fluorophores with aggregation-induced emission (AIE) properties by Tang and coworkers accessed a virtual toolbox of building blocks, which widely explores the luminescent materials [8,9]. The development of non-covalent-mediated supramolecular chemistry provides a promising tool to control the assembly mode of building blocks, endowing programmable multicolor fluorescence [10–15]. As a result, various luminescent materials with color-tunable, intensity (quantum yield)-controllable, lifetime-desirable properties have been developed, showing potential applications in information encryptions, fluorescent sensors, and imaging probes [16–23].

To further develop advanced luminescent materials, two challenges should be considered: (i) most multicolor fluorescence materials focus on integrating various fluorophores into one system, which is not only difficult to precisely control luminescence owing to undesirable inter/intramolecular interactions but also accompanied by tremendous cost and environmental drawbacks. Constructing white-light-including multicolor luminescent materials based on single fluorophore is therefore essential but difficult to achieve owing to the limit of luminescent properties of single fluorophore; (ii) manipulating molecular assembly switches between different thermodynamically stable states and hence resulting in switchable fluorescence is a deep understanding for chemists. How to control molecular assembly in a biomimetic manner to push assemblies far away from the thermodynamics equilibrium state [24–28], achieving dynamic timing control over multicolor fluorescence?

Up to now, much effort has been devoted to developing smart luminescent materials [29–33]. For example, Stoddart and coworkers constructed a multicolor fluorescence system in which fluorescence can be tuned from blue to green and yellow by thermodynamically controlling the formation of host-guest complexes based on single fluorophore [11]. An ATP-driven hydrogel displaying blue circularly polarized luminescence on time scale was developed by Liu and coworkers [30]. Our group also achieved dynamic timing control over tunable fluorescence (yellow and purple) by controlling individual molecular conformation [31]. These works showed remarkable progress in color-tunable luminescent materials, addressing one of the abovementioned challenges. However, both, *i.e.*,

* Corresponding authors.
E-mail addresses: P0586@ecust.edu.cn (Q. Wang), dahui_qu@ecust.edu.cn (D.-H. Qu).
[1] These authors contributed equally to this work.

https://doi.org/10.1016/j.cclet.2023.108972
1001-8417/

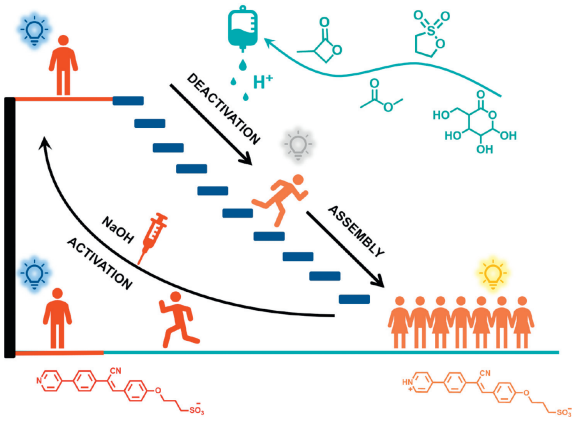

Fig. 1. Molecular structures and schematic representation of temporal-controlled assembly system with time-dependent multicolor fluorescence.

achieving time-dependent white-light-including multicolor fluorescence by controlling the activation and deactivation of single motif on time scale is still rarely reported.

Herein, such material is developed through integrating pH-responsive molecule to a pH-dependent system constructed by activators (NaOH) and deactivators (esters). An alkaline solution that automatically revert back to acid condition with time can be created by introducing both activators and deactivators in the meantime (Fig. 1). As a result, time-dynamic molecular assembly occurrs, resulting in multicolor fluorescence, which automatically changes from blue to white and yellow with time. Taking advantage of the dynamic fluorescence, advanced information encryption materials, fluorescent ink, three-dimension (3D) code and even time-dependent 3D code (four-dimension code, 4D code) are developed, enabling multiple level information encryption, which efficiently improves information security.

The molecular structure of compound **1** was confirmed by nuclear magnetic resonance (NMR) and mass spectrometry (Figs. S2–S4 in Supporting information). To investigate the pH responsive property (Fig. 2a), ^{1}H NMR was performed (Fig. 2b). The upshift fielded of the proton signals $H_{a,b}$ indicated the protonation of pyridine moiety. This protonation may result in the red-shifted of the optical properties. Therefore, the ultraviolet and visible (UV–vis) absorption spectra of various pH aqueous solutions was carried out (Fig. 2c). Rather than a considerable red-shift absorption, the absorbance showed a dramatic decrease at 365 nm and an increase above 400 nm in aqueous solution (pH 5). A turbid solution was observed when the solution's pH changes from 6 to 5. These results suggested the assembly of compound **1** in acid condition. The assembly behavior was also confirmed by the change of zeta potential and the diameter of the assemblies was revealed by dynamic light scattering (DLS) (Fig. S5 in Supporting information). The formation of this abnormal assembly may be attributed to the intermolecular electronic interactions between the sulfonic group and the protonated pyridine moiety.

The assembly behavior resulted in a distinctive change in the fluorescence. Weak fluorescence at 450 nm in aqueous solution (pH 6–12) was observed, which dramatically increased when pH changed from 6 to 5 (Fig. 2d). Furthermore, the absolute quantum yield was carried out (Fig. S6 in Supporting information), revealing 42% for the assemblies while only 0.25% for the solution (pH 12). The change in the fluorescent color was presented in Commission Internationale d'Eclairage (CIE) chromaticity coordinates, showing a gradual change from blue (0.20, 0.21) to yellow (0.40, 0.52) with a pH decrease (Fig. S7 in Supporting information). The assembly also resulted in an increase in the fluorescence lifetime (Fig. S8 in Supporting information). Optical microscopy was employed to investigate the morphologies of the assemblies (Fig. S9 in Supporting information). Small particles with orange fluorescence were observed in the dark, and moreover, the bright pattern was observed in the polarized field, suggesting the presence of ordered crys-

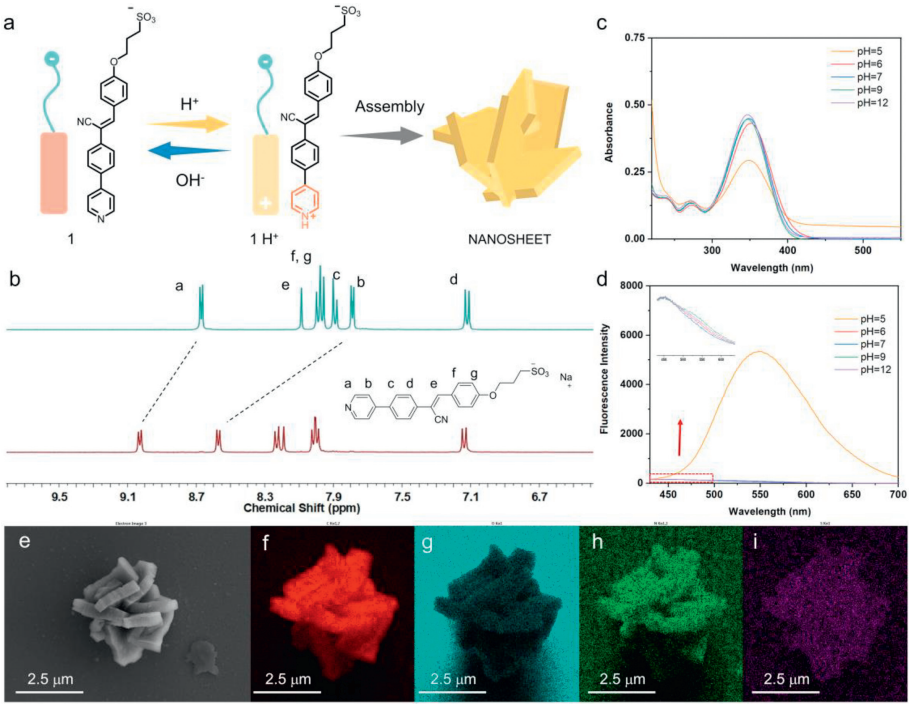

Fig. 2. pH-dependent molecular assembly. (a) A schematic illustration of the pH-controlled assembly process. (b) ^{1}H NMR (DMSO-d_6) spectra of compound **1** (5 mmol/L) prior (green line) and after (red line) addition of hydrochloric acid. (c) UV–vis absorption spectra of the compound **1** in aqueous solutions under different pH values. (d) The fluorescence spectra of compound **1** aqueous solutions under different pH values. (e) SEM images of nanosheet assemblies and corresponding elemental mapping images of (f) carbon, (g) oxygen, (h) nitrogen, and (i) sulfur elements.

talline structures. Scanning electron microscopy (SEM) was further carried out, revealing nanosheet morphologies with good mapping with carbon, oxygen, nitrogen and sulfur elements (Figs. 2e–i).

Taking advantage of this pH-induced assembly feature, we investigated whether the molecular assembly can be controlled on time scale and further developed a biomimic non-equilibrium system. Our strategy was integrating an ester-hydrolysis resection to this pH-trigger assembly system (Fig. 3a). Once the promoters (NaOH) and deactivators (esters) were introduced to the solution, a transient alkaline solution was achieved, which automatically reverted back to acid condition with time, leading to molecular assembly on time scale.

The hydrolysis process of the cyclic ester, β-butyrolactone, was monitored by pH meter, showing a dramatical decrease from pH 11.5 to pH 6 and a slow change from pH 6 to pH 5 (Fig. 3b). A similar change was observed in the presence of compound **1**, suggesting the hydrolysis process cannot be affected by compound **1**. During this time-dependent process, we noticed that the pH range with slow kinetics matches the range of pyridine protonation, creating an optimized condition to perform self-assembly on time scale. To investigate the assembly behaviors, UV–vis spectra was carried out (Fig. 3c). After introducing β-butyrolactone to an aqueous solution of compound **1**, the absorption peak at 350 nm automatically decreased while the absorbance at 410 nm gradually increased with time, indicating the occurrence of assembly with time. This time-dependent assembly turned on the time-gated fluorescence, recorded by the fluorescence spectra (Fig. 3d). The fluorescence emission peak at 550 nm gradually increased with time and reached equilibrium at about 45 min. The plot of the absorbance and fluorescence intensity at 550 nm *versus* time revealed a similar transition process (Fig. S10 in Supporting information). Moreover, the fluorescence color change was recorded by the CIE 1931 chromaticity diagram and fluorescent images (Figs. 3e and f), showing time-dependent changing from blue (0.19, 0.20) to white (0.29, 0.33) and yellow (0.42, 0.52). The morphology was further investigated by optical microscopy (Fig. S11 in Supporting information) and SEM (Figs. 3g–k), revealing the rod-like assemblies, which were different from the assemblies generated by direct treatment with acid.

The time-dependent assembly process can be controlled by regulating some parameters such as ester concentrations, temperature, initial pH value, and stirring rate (Fig. S12 in Supporting information). Higher concentrations resulted in a faster process with shorter $t_{1/2}$ (0.06 mmol, 32 min), while a slower process with longer $t_{1/2}$ was observed when using 0.06 mmol β-butyrolactone. Temperature was another important parameter to control the hydrolysis process. The increase in temperature (from 15 °C to 40 °C) led to decreasing $t_{1/2}$ (from 130 min to 40 min), which may be attributed to the faster hydrolysis rate of the ester. The initial pH value mainly affects the lag time. In an alkaline solution (pH 12), a distinctive lag time was observed after introducing β-butyrolactone while it became shorter at pH 10 and un-detectable at pH 7. In other words, once β-butyrolactone was introduced into a neutral aqueous solution of compound **1**, the assembly occurred in a short period of time. In addition, the hydrolysis process can be accelerated by mechanical agitation such as stirring, as this facilitates the dispersion of β-butyrolactone. The assembly cannot occur under 0 revolutions per minute (r.p.m) condition

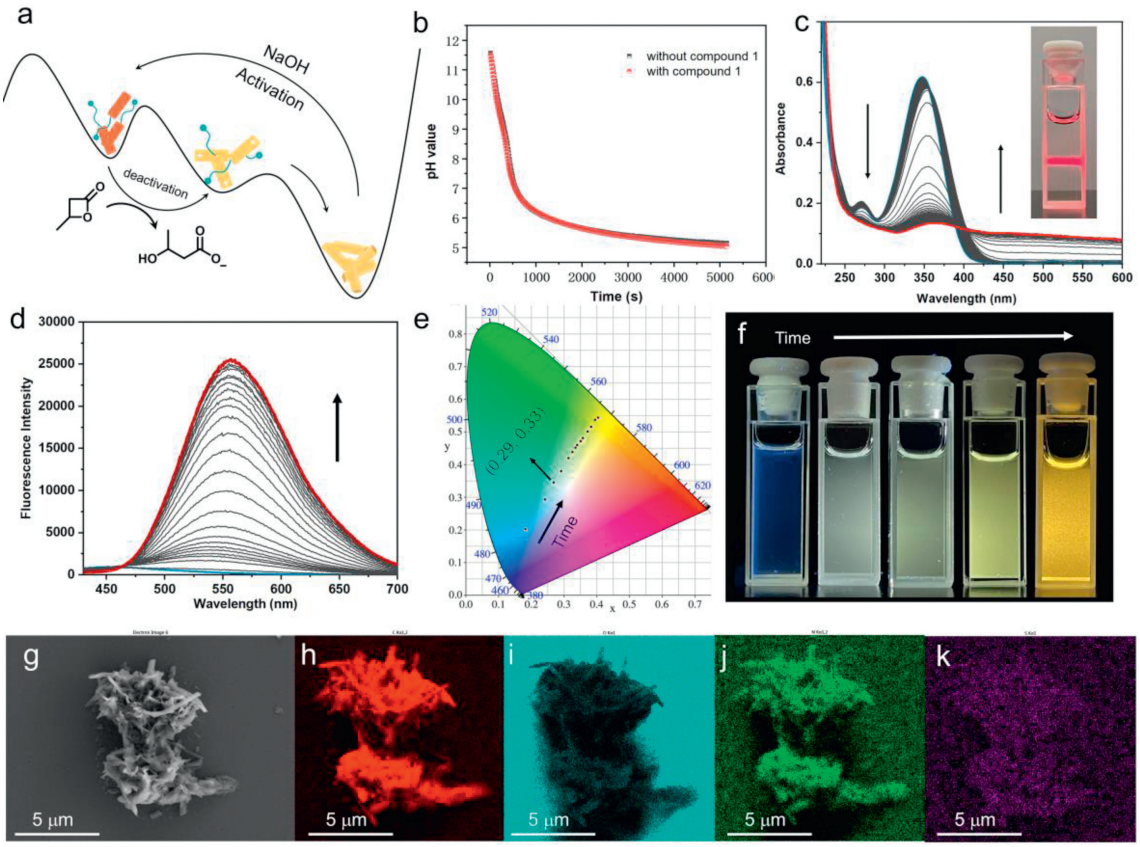

Fig. 3. Time-dependent molecular assembly. (a) A schematic illustration of the time-dependent assembly process. (b) Influence of the compound on pH changes of the solution after adding 0.15 mmol β-butyrolactone (stirring rate: 300 r.p.m.). Time-dependent (c) UV–vis absorption and (d) fluorescence spectra of compound **1** in aqueous solutions after introducing 0.24 mmol β-butyrolactone (initial pH 12, stirring rate: 300 r.p.m.). (e) Time-dependent CIE coordinate diagram corresponding to d, showing the fluorescent color change from blue to yellow with time. (f) A series of fluorescent images of the time-dependent multicolor fluorescence. (g) SEM images of nanosheet assemblies and corresponding elemental mapping images of (h) carbon, (i) oxygen, (j) nitrogen, and (k) sulfur elements.

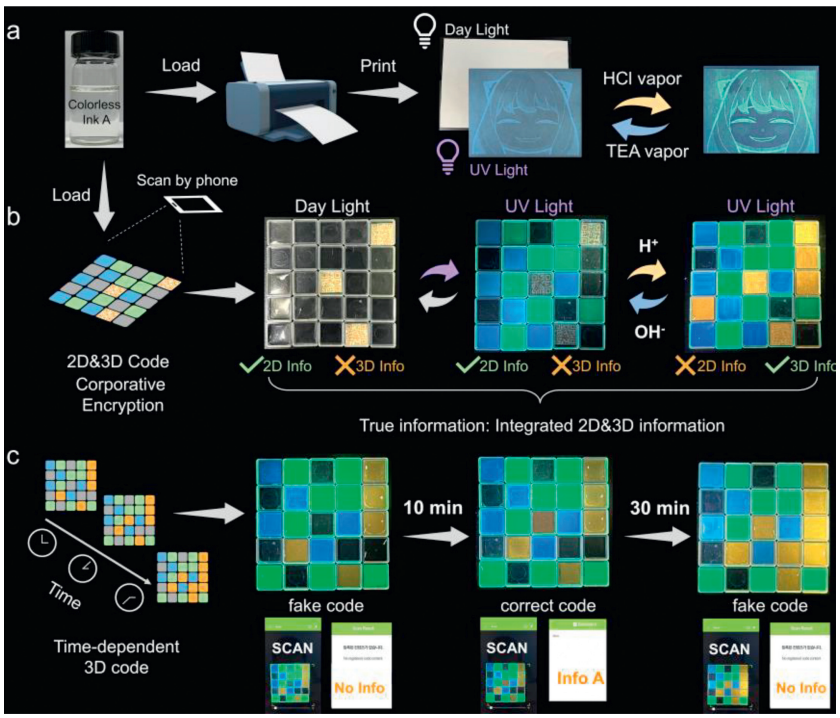

Fig. 4. Dynamic information encryption materials. (a) Schematic representations for the printing experiment using colorless compound **1** solution as ink and fluorescence images of the printing pattern before and after treatment with acid/base. (b) Schematic representations for the integration of 2D codes and fluorescent 3D code and a series of codes under different conditions. (c) Schematic representations and photographs of the time-dependent 3D codes.

because β-butyrolactone was precipitated in the bottom, and the hydrolysis period was too long to observe. However, a transparent solution with good dispersion of the ester was achieved when the stirring rate was above 300 r.p.m. In this situation, the hydrolysis process was dependent on other parameters that we discussed above instead of the dispersion. Therefore, the assembly was triggered and showed a similar change process under 300 r.p.m and 600 r.p.m. Other esters, such as methyl formate, δ-lactone, and 1,3-propanesultone, were also introduced to explore the diversity and general suitability of the timing-controlled assembly process (Fig. S13 in Supporting information), showing similar behaviors with different $t_{1/2}$.

Taking advantage of the dynamic fluorescent feature, the compound solution was further developed into fluorescent ink for information encryption (Fig. 4a). The printed pattern was invisible in daylight owing to colorless ink, while it exhibited blue fluorescence under UV light, which turned to yellow fluorescence after introducing acid vapor. Such fluorescence change was reversible. The yellow fluorescence reverted to blue after treatment with triethylamine (TEA) vapor (Fig. S14 in Supporting information). Compared to those static anti-configurations fluorescent ink, such dynamic property provided the second encryption level for information.

This result further encouraged us to develop an advanced information encryption material, fluorescent 3D code (Fig. 4b), where information was encoded in three types of fluorescence color instead of black and white (2D code). Moreover, the 2D code was integrated into the 3D code to achieve multiple level information encryption. The fluorescent 3D code was comprised of the aqueous solutions of pyrenesulfonate (blue color), pyranine (green color), and compound **1** (yellow color). These solutions were transparent under daylight and hence only 2D code can be recognized by a smart-phone (first encryption). Two fluorescence colors, blue and green, were turned on under UV light, while the other was still invisible due to its weak quantum yield in solution. In this situation, the 3D code was still unrecognizable (second encryption). Treatment with small amount of acid solutions turned on the yellow fluorescence and led to a turbid solution. Therefore, the 2D code was hidden, and only 3D code information can be recognized (third encryption). This property endowed the selective recognition of the information. True information must be decrypted by integrating the 2D code and 3D code.

Additionally, we explored whether the time dimension can be introduced to 3D code to endow materials with time-dependent features, achieving advanced information encryption. As demonstrated above, β-butyrolactone was promising for controlling molecular assembly on time scale, resulting in time-dependent yellow fluorescence. Taking advantage of this feature, various concentrations of β-butyrolactone were introduced to temporal control the appearance of yellow fluorescence. A series of information ("0", "2", "8") was successfully controlled to display on time scale by regulating β-butyrolactone concentrations (Fig. S15 in Supporting information). Based on this result, time-dependent 3D code (4D code) was further developed. The ester concentration in the middle box (3, 3) was 0.029 mol/L (Fig. S16 in Supporting information), while the (4, 2) and (5, 1) were 0.12 mol/L, leading to time-gate fluorescence. As a result, series of codes were generated on time scale, while the correct one with information A only can be recognized at 10 min (Fig. 4c). Otherwise, fake codes with no information were presented. This time-dependent encryption feature endowed materials with high-level security.

In summary, the temporal control of assembly was achieved by integrating a hydrolysis reaction to a pH-trigger assembly system. Compound 1 existed in monomeric state in aqueous solution with weak fluorescence, which assembled to yellow fluorescent nanosheet after being treated with hydrochloric acid. The assembly behavior can be controlled on time scale by introducing esters as deactivators, leading to nanorod assemblies with time-dependent multicolor fluorescence automatically changing from blue to white and yellow. The kinetic assembly process was controlled by tuning

temperature, ester concentration, initial pH and stirring rate. Taking advantage of this dynamic feature, fluorescent ink and 3D code were developed to achieve multiple level information encryption. Moreover, time-dependent fluorescent 3D code, an advanced information encryption material with time-dependent security, was developed, showing multiple pieces of information on a time scale and the correct one can be identified at only a specified time. We hope this work, on the one hand, motivates the fabrication of biomimic non-equilibrium system in which molecular assembly was performed in a spatial and temporal controlled manner; on the other hand, it inspires the development of advanced information encryption materials based on smart fluorescent systems.

Tailoring luminescent properties on time scale is a key research objective but remains a challenge. Controlling molecular assembly on time scale was achieved by integrating a pH-responsive motif to a transient alkaline solution fabricated by activators and deactivators, leading to time-dependent multicolor fluorescence changing from blue to white and yellow.

Declaration of competing interest

The authors declare that they have no known competing financial interests or personal relationships that could have appeared to influence the work reported in this paper.

Acknowledgments

This work was supported by the National Natural Science Foundation of China (Nos. 22220102004, 22025503), Shanghai Municipal Science and Technology Major Project (No. 2018SHZDZX03), the Innovation Program of Shanghai Municipal Education Commission (No. 2023ZKZD40), the Fundamental Research Funds for the Central Universities, the Programme of Introducing Talents of Discipline to Universities (No. B16017), Science and Technology Commission of Shanghai Municipality (No. 21JC1401700), and the Starry Night Science Fund of Zhejiang University Shanghai Institute for Advanced Study (No. SN-ZJU-SIAS-006).

Supplementary materials

Supplementary material associated with this article can be found, in the online version, at doi:10.1016/j.cclet.2023.108972.

References

[1] H. Nie, Z. Wei, X.L. Ni, Y. Liu, Chem. Rev. 122 (2022) 9032–9077.
[2] T. Higuchi, H. Nakanotani, C. Adachi, Adv. Mater. 27 (2015) 2019–2023.
[3] Z.C. Jiang, Y.Y. Xiao, J.B. Hou, et al., Angew. Chem. Int. Ed. 61 (2022) e202211959.
[4] R. Kotani, S. Yokoyama, S. Nobusue, et al., Nat. Commun. 13 (2022) 303.
[5] R. Wang, W. Lu, Y. Zhang, et al., Chin. Chem. Lett. 34 (2023) 108086.
[6] K. Yang, B. Yu, W. Liu, et al., Chin. Chem. Lett. 34 (2023) 107889.
[7] T. Zhang, X. Chen, C. Yuan, et al., Angew. Chem. Int. Ed. 62 (2023) e202211550.
[8] J. Luo, Z. Xie, J.W.Y. Lam, et al., Chem. Commun. (2001) 1740–1741.
[9] S. Qin, H. Zou, Y. Hai, L. You, Chin. Chem. Lett. 33 (2022) 3267–3271.
[10] A. Aliprandi, M. Mauro, L. De Cola, Nat. Chem. 8 (2016) 10–15.
[11] H. Wu, Y. Wang, L.O. Jones, et al., J. Am. Chem. Soc. 142 (2020) 16849–16860.
[12] B. Lin, Q. Wang, Z. Qi, H. Xu, D.H. Qu, Sci. China Chem. 66 (2023) 1111–1119.
[13] Y. Ai, M.H.Y. Chan, A.K.W. Chan, et al., Proc. Natl. Acad. Sci. U. S. A. 116 (2019) 13856–13861.
[14] Q. Li, H. Zhang, K. Lou, et al., Proc. Natl Acad. Sci. U. S. A. 119 (2022) e2121746119.
[15] Q. Wang, B. Lin, M. Chen, et al., Nat. Commun. 13 (2022) 4185.
[16] A. Ghosh, I. Paul, M. Schmittel, J. Am. Chem. Soc. 143 (2021) 5319–5323.
[17] H. Wu, Y. Chen, X. Dai, et al., J. Am. Chem. Soc. 141 (2019) 6583–6591.
[18] Z. Cao, D. Wu, M. Li, et al., Chin. Chem. Lett. 33 (2022) 1533–1536.
[19] Z.T. Shi, Q. Wang, J. Yi, et al., Angew. Chem. Int. Ed. 61 (2022) e202207405.
[20] J. Du, L. Sheng, Y. Xu, et al., Adv. Mater. 33 (2021) 2008055.
[21] Q. Wang, Z. Qi, Q.M. Wang, et al., Adv. Funct. Mater. 32 (2022) 2208865.
[22] W.H. Jin, Q. Wang, M. Chen, Q. Zhang, D.H. Qu, Mater. Chem. Front. 5 (2021) 2347–2352.
[23] Y. Wang, H. Wu, W. Hu, J.F. Stoddart, Adv. Mater. 34 (2022) 2105405.
[24] J.H. van Esch, R. Klajn, S. Otto, Chem. Soc. Rev. 46 (2017) 5474–5475.
[25] M. Weißenfels, J. Gemen, R. Klajn, Chem 7 (2021) 23–37.
[26] Q. Wang, Z. Qi, M. Chen, D.H. Qu, Aggregate 2 (2021) e110.
[27] J. Boekhoven, W.E. Hendriksen, G.J.M. Koper, R. Eelkema, J.H. van Esch, Science 349 (2015) 1075–1079.
[28] B. Rieß, R.K. Grötsch, J. Boekhoven, Chem 6 (2020) 552–578.
[29] Q. Wang, Q. Zhang, Q.W. Zhang, et al., Nat. Commun. 11 (2020) 158.
[30] H. Fan, K. Li, T. Tu, et al., Angew. Chem. Int. Ed. 61 (2022) e202200727.
[31] Z. Zong, Q. Zhang, S.H. Qiu, et al., Angew. Chem. Int. Ed. 61 (2022) e202116414.
[32] Z. Li, X. Ji, H. Xie, B.Z. Tang, Adv. Mater. 33 (2021) 2100021.
[33] Z. Li, X. Liu, G. Wang, et al., Nat. Commun. 12 (2021) 1363.